

# Extended colored Zee-Babu model

Takaaki Nomura<sup>1,\*</sup> and Hiroshi Okada<sup>2,†</sup>

<sup>1</sup>School of Physics, KIAS, Seoul 130-722, Korea

<sup>2</sup>Physics Division, National Center for Theoretical Sciences, Hsinchu 300, Taiwan

(Received 31 July 2016; published 28 October 2016)

We study the extended colored Zee-Babu model introducing a vectorlike quark and singlet scalar. The active neutrino mass matrix and muon anomalous magnetic moment, which can be fitted to experimental data satisfying the constraints from the flavor-changing neutral current, are analyzed. Then, we discuss the constraint from  $h_{\text{SM}} \rightarrow \gamma\gamma$ , the implication of an exotic diphoton resonance as a signature of the model, and the stability of the scalar potential. In addition, we discuss the signature of our model via vectorlike quark production.

DOI: 10.1103/PhysRevD.94.075021

## I. INTRODUCTION

Radiative seesaw models are one of the interesting possibilities not only to generate active neutrino masses but also to explain some phenomenological viewpoints such as the muon anomalous magnetic moment  $[(g - 2)_\mu]$  and dark matter candidate,<sup>1</sup> which have not been uncovered yet. Furthermore, these particles can be correlated with each other. Thus, following vintage papers at one-loop, two-loop, and three-loop models that are, respectively, found in Refs. [1,2], and [3], a vast amount of literature has recently arisen along this idea [4] at one-loop level, [5] at two-loop level, [6] at three-loop level, and [7,8] at four-loop level. In many cases, neutrino mass is generated via a loop diagram associated with colorless particles. However, colored particles also can propagate inside a loop diagram in neutrino mass generation, which would provide other phenomenologically interesting effects.

In 2015, the excess of events in the diphoton channel was announced by both the ATLAS and CMS collaborations at the LHC 13 TeV where the invariant mass of the diphoton is  $m_{\gamma\gamma} \simeq 750$  GeV [9,10]. This diphoton resonance could be considered as a spin-0 or -2 particle decaying into a diphoton, the earlier works to interpret the excess of which can be found in, e.g., Refs. [11–43]. In 2016, however, new LHC data of the diphoton resonance search which disfavors the excess was announced [44–46]. Although the diphoton excess is more like statistical fluctuations, the studies on this issue have shown that the diphoton resonance search can be an interesting probe of a scalar (or pseudoscalar) boson interacting with fields having color and/or electric charge.

In this paper, we extend the colored Zee-Babu model proposed in Ref. [47] by including an isosinglet vectorlike quark and a standard model (SM) singlet scalar field to explain  $(g - 2)_\mu$ . The active neutrino matrix and  $(g - 2)_\mu$  are induced at two-loop and one-loop levels. We then analyze them, taking into account the constraints from the flavor-changing neutral current (FCNC). Moreover, we discuss implications to the scalar sector including the exotic diphoton resonance search. In addition, implications to collider physics in which we focus on the signature of newly introduced vectorlike quark are discussed.

This paper is organized as follows. In Sec. II, we show our model, including the neutrino sector,  $(g - 2)_\mu$ , and constraints from the FCNC. The scalar sector is investigated in Sec. III, including diphoton decay of the SM Higgs, exotic diphoton resonance, and potential stability. In Sec. IV, we discuss some implications of our model for collider physics. We conclude and discuss in Sec. V.

## II. MODEL SETUP AND ANALYSIS

We devote this section to reviewing our model. Our field contents and their charge assignments are the same as the original colored Zee-Babu model proposed by the Kohda, Sugiyama, and Tsumura group in Ref. [47] except for the vectorlike quark  $Q'$  with an  $SU(2)_L$  singlet and a gauge singlet boson  $\varphi$ . We show all the field contents and their charge assignments in Table I for the fermion sector and Table II for the boson sector. Here,  $\varphi$  is introduced to illustrate the effect of the diquark, leptoquark, and vectorlike quark on exotic diphoton resonance from a new neutral scalar boson. The main motivation to introduce  $Q'$  is to explain the sizable  $(g - 2)_\mu$ .<sup>2</sup> Under this framework, the renormalizably relevant Lagrangian is given by

\*nomura@kias.re.kr

†macokada3hiroshi@cts.nthu.edu.tw

<sup>1</sup>In this paper, dark matter candidates are not included.

<sup>2</sup>We have checked that the original model cannot obtain the sizable discrepancy of  $(g - 2)_\mu$  from the SM.

TABLE I. Field contents of fermions and their charge assignments under  $SU(3)_C \times SU(2)_L \times U(1)_Y$ , where the lower index  $i (= 1 - 3)$  represents the number of flavors.

Quarks			Leptons		
$Q_{L_i}$	$u_{R_i}$	$d_{R_i}$	$Q'$	$L_{L_i}$	$e_{R_i}$
$SU(3)_C$	<b>3</b>	<b>3</b>	<b>3</b>	<b>3</b>	<b>1</b>
$SU(2)_L$	<b>2</b>	<b>1</b>	<b>1</b>	<b>1</b>	<b>2</b>
$U(1)_Y$	$\frac{1}{6}$	$\frac{2}{3}$	$-\frac{1}{3}$	$-\frac{4}{3}$	$-\frac{1}{2}$

$$\begin{aligned} -\mathcal{L} = & (y_\ell)_{ij} \bar{L}_L \Phi e_{R_j} + (y_L)_{ij} \bar{L}_{L_i}^c (i\sigma_2) Q_{L_j} S_{LQ}^* \\ & + (y_R)_{ij} \bar{e}_{R_i}^c u_{R_j} S_{LQ}^* + (y_S)_{ij} \bar{d}_{R_i}^c d_{R_j} S_{DQ}^* \\ & + Y_i \bar{e}_{R_i} Q'_L S_{LQ}^* + m_{Q'} \bar{Q}' Q' + \text{H.c.}, \end{aligned} \quad (2.1)$$

where  $\sigma_2$  is the second component of the Pauli matrix, and the second line is the new terms. Since the potential associated with the leptoquark and diquark is trivial, we abbreviate the explicit expression; see the original paper [47] for details. Here, we show the potential for  $\Phi$  and  $\varphi$ , which determines the vacuum expectation values (VEVs) of them:

$$\begin{aligned} V \supset & \mu^2 \Phi^\dagger \Phi + \lambda (\Phi^\dagger \Phi)^2 + m_\varphi^2 \varphi^2 + \mu_\varphi \varphi^3 + \lambda_\varphi \varphi^4 \\ & + \mu_\varphi \Phi \varphi (\Phi^\dagger \Phi) + \lambda_\varphi \Phi \varphi^2 (\Phi^\dagger \Phi) \\ & + (\text{terms containing leptoquark and diquark}). \end{aligned} \quad (2.2)$$

The Higgs doublet  $\Phi$  and singlet  $\varphi$  are written by

$$\Phi = \begin{pmatrix} G^+ \\ \frac{1}{\sqrt{2}}(v + \tilde{h} + iG^0) \end{pmatrix}, \quad \varphi = \frac{1}{\sqrt{2}}(v_\varphi + \phi), \quad (2.3)$$

where  $G^+$  and  $G^0$  are the Goldstone bosons,  $\tilde{h}$  is the SM-like Higgs field, and  $v(v_\varphi)$  is the VEVs of  $\Phi$  ( $\varphi$ ). Then, applying the minimal conditions  $\partial V(v, v_\varphi)/\partial v = 0$  and  $\partial V(v, v_\varphi)/\partial v_\varphi = 0$ , we obtain the stable VEVs such that

$$\begin{aligned} \mu^2 + \lambda v^2 + \frac{\lambda_{\varphi\Phi}}{2} v_\varphi^2 + \frac{\mu_{\varphi\Phi}}{\sqrt{2}} v_\phi &= 0, \\ m_\varphi^2 v_\varphi + \frac{3\mu_\varphi v_\varphi^2}{2\sqrt{2}} + \frac{\mu_{\varphi\Phi} v^2}{2\sqrt{2}} + \lambda_\varphi v_\varphi^3 + \frac{\lambda_{\varphi\Phi} v_\varphi v^2}{2} &= 0. \end{aligned} \quad (2.4)$$

TABLE II. Field contents of bosons and their charge assignments under  $SU(3)_C \times SU(2)_L \times U(1)_Y$ .

	$\Phi$	$\varphi$	$S_{LQ}^a$	$S_{DQ}^{ab}$
$SU(3)_C$	<b>1</b>	<b>1</b>	<b>3</b>	<b>6</b>
$SU(2)_L$	<b>2</b>	<b>1</b>	<b>1</b>	<b>1</b>
$U(1)_Y$	$\frac{1}{2}$	0	$-\frac{1}{3}$	$-\frac{2}{3}$

In our analysis, we assume  $v_\varphi \ll v, m_\varphi$  so that the VEVs are approximated to  $v \simeq \sqrt{-\mu^2/\lambda}$  and  $v_\varphi \simeq -\mu_{\varphi\Phi} v^2 / (\sqrt{2}(2m_\varphi^2 + \lambda_{\varphi\Phi} v^2))$ . Taking  $|\mu_{\varphi\Phi}| \sim O(1)$  GeV, we can suppress mixing between the SM Higgs and the singlet scalar to be consistent with experimental data regarding the SM Higgs [48,49]. In the following analysis, we ignore the mixing effect.

### A. Neutrino sector

The neutrino mass matrix is induced at the two-loop level as can be seen in the original paper [47], and its formula is given by

$$\mathcal{M}_{\nu_{ab}} \approx \frac{24\mu}{(4\pi)^4 m_{LQ}^2} \mu (y_L^*)_{ai} m_{d_i} (y_S)_{ij} m_{d_j} (y_L^\dagger)_{jb} F_1(r), \quad (2.5)$$

$$F_1(r) = \int_0^1 dx \int_0^{1-x} dy \frac{1}{x + y(-1 + y + r^2)} \ln \left[ \frac{x + r^2 y}{y - y^2} \right], \quad (2.6)$$

where  $\mu$  comes from the term of  $S_{LQ}^* S_{LQ}^* S_{DQ}$ ,  $r \equiv (m_{DQ}/m_{LQ})^2$ , and we have assumed that the down-quark masses in the loop are negligible compared to the masses of leptoquark and diquark bosons. Notice here that  $F_1(r)$  is solved only through the numerical way, even though an approximated analytical formula is known in the limit of  $r \ll 1$  or  $r \gg 1$  [50]. Neutrino oscillation data are given by diagonalizing  $\mathcal{M}_{ab}$  as

$$\mathcal{M}_\nu^{\text{diag}} = V_{\text{MNS}}^T \mathcal{M}_\nu V_{\text{MNS}}, \quad (2.7)$$

where  $V_{\text{MNS}}$  is the Maki-Nakagawa-Sakata mixing matrix of the neutrino. For experimental values, we adopt the best-fit values with the global analysis in Ref. [51],

$$\begin{aligned} s_{12}^2 &= 0.323, & s_{23}^2 &= 0.567, \\ s_{13}^2 &= 0.0234, & \delta_{CP} &= 1.34\pi, \\ |m_{\nu_3}^2 - m_{\nu_2}^2| &= 2.48 \times 10^{-3} \text{ eV}^2, \\ m_{\nu_2}^2 - m_{\nu_1}^2 &= 7.60 \times 10^{-5} \text{ eV}^2, \end{aligned} \quad (2.8)$$

where we assume one of the three neutrino masses is zero with normal ordering for simplicity in the numerical analysis below.

### B. Flavor changing neutral currents lepton flavor violations

Before discussing the FCNCs and the lepton flavor violations (LFVs), we specify the textures of  $y_L$  and  $y_S$  to evade some FCNC processes. In this paper, we adopt the textures

$$y_L = V_{\text{MNS}} \times y'_L \equiv V_{\text{MNS}} \times \begin{bmatrix} (y_L)_{11} & 0 & 0 \\ 0 & (y_L)_{22} & (y_L)_{23} \\ 0 & (y_L)_{32} & (y_L)_{33} \end{bmatrix},$$

$$y_S = \begin{bmatrix} 0 & 0 & 0 \\ 0 & (y_S)_{22} & (y_S)_{23} \\ 0 & (y_S)_{23} & (y_S)_{33} \end{bmatrix}, \quad (2.9)$$

where  $y_S$  is a symmetric matrix. Then, the neutrino mass formula can be simplified as follows:

$$\mathcal{M}_\nu^{\text{diag}} = V_{\text{MNS}}^T \mathcal{M}_\nu V_{\text{MNS}} = y_L'^* \omega y_L'^\dagger, \quad (2.10)$$

$$\omega \equiv \frac{24\mu}{(4\pi)^4 m_{LQ}^2} m_d y_S m_d F_1(r). \quad (2.11)$$

From Eq. (2.10), one finds that  $(y_S)_{23}$  is identically zero.

Here, we discuss the FCNCs and the LFVs, where we focus on terms related to the neutrino masses, that is,  $y_L$  and  $y_S$ . Notice here that the constraint on  $K^0 - \bar{K}^0$  mixing and  $B_d^0 - \bar{B}_d^0$  mixing can be evaded if we take  $(y_S)_{11} = 0$ .

Thus, the bound on LFVs comes from the  $\mu - e$  conversion and  $\ell_i \rightarrow \ell_j \gamma$  process, and the bounds on FCNCs come from  $K^+ \rightarrow \pi^+ \nu \bar{\nu}$  and  $D^+ \rightarrow \pi^+ \mu^+ \nu^-$  decays and the  $Q - \bar{Q}$  mixing, where  $Q = K^0, B_s^0$ . These are, respectively, constrained by the combinations [52]

$$\mu - e \text{ conversion: } \left| \frac{(y_L)_{21}(y_L^\dagger)_{11}}{4\sqrt{2}G_F m_{LQ}^2} \right| \lesssim 8.5 \times 10^{-7}, \quad (2.12)$$

$$\ell_i \rightarrow \ell_j \gamma: \left| \frac{3\alpha_{em}|(y_L y_L^\dagger)_{ij}|^2 C_i}{256\pi G_F^2 m_{LQ}^4} \right| \lesssim (4.2 \times 10^{-13}, 3.3 \times 10^{-8}, 4.4 \times 10^{-8}),$$

for  $(i, j) = [(\mu, e), (\tau, e), (\tau, \mu)]$ , (2.13)

$$K^+ \rightarrow \pi^+ \nu \bar{\nu}: \left| \sum_{i,j}^{1-3} \frac{(y_L)_{i2}(y_L^\dagger)_{1j}}{4\sqrt{2}G_F m_{LQ}^2} \right| \lesssim 9.4 \times 10^{-6}, \quad (2.14)$$

$$D^+ \rightarrow \pi^+ \mu^+ \mu^-: \left| \frac{(y_L)_{21}(y_L^\dagger)_{22}}{4\sqrt{2}G_F m_{LQ}^2} \right| \lesssim 6.1 \times 10^{-3}, \quad (2.15)$$

$$B_s^0 - \bar{B}_s^0 \text{ mixing: } \left| \frac{(y_S)_{22}(y_S^\dagger)_{33}}{G_F m_{DQ}^2} \right| \lesssim 3.3 \times 10^{-10}, \quad (2.16)$$

where  $C_i \approx (1, 1/5)$  for  $(\mu, \tau)$ . For numerical analysis, we will impose the above constraints.

### C. Muon anomalous magnetic moment $(g - 2)_\mu$

First of all, the original paper suggests that the term through  $y_L$  cannot induce the sizable  $(g - 2)_\mu$ , assuming  $y_R$

to be zero. However, we find that  $y_R$  cannot contribute to  $(g - 2)_\mu$  even the case of  $y_R \neq 0$  because of an accidental electric charge cancellation in the limit of massless mediating up-type quarks,

$$\Delta a_\mu(y_R) \propto 2Q_{S_{LQ}} + Q_{u_k} = 2 \times \left( -\frac{1}{3} \right) + \frac{2}{3} = 0. \quad (2.17)$$

Thus, we rely on the new source as a new term  $Y$ , and its form is given by

$$\Delta a_\mu(T) = Y_2^\dagger Y_2 m_\mu^2 (G_1[m_{Q'}, m_{LQ}] + 4G_1[m_{LQ}, m_{Q'}]), \quad (2.18)$$

$$G_1[m_1, m_2] = \frac{1}{24m_1^2}, \quad \text{for } m_1 = m_2, \quad (2.19)$$

$$G_1[m_1, m_2]$$

$$= \frac{2m_1^6 + 3m_1^4 m_2^2 - 6m_1^2 m_2^4 + m_2^6 + 12m_1^4 m_2^2 \ln(\frac{m_2}{m_1})}{12(m_1^2 - m_2^2)^4},$$

for  $m_1 \neq m_2$ . (2.20)

Also, we have to consider the lepton flavor processes through this term. Here, we impose the constraints of  $\ell_i \rightarrow \ell_j \gamma$ , and its branching ratio (BR) is given by

$$\text{BR}(\ell_i \rightarrow \ell_j \gamma) = \frac{48\pi^3 \alpha_{em} C_i}{G_F^2} Y_i^\dagger Y_j |G_1[m_{Q'}, m_{LQ}] + 4G_1[m_{LQ}, m_{Q'}]|^2, \quad (2.21)$$

where  $\alpha_{em}$  is the fine structure constant and  $G_F$  is the Fermi constant. The experimental bound for  $\text{BR}(\ell_i \rightarrow \ell_j \gamma)$  is the same as the one in Eq. (2.13).

### D. Result of numerical analysis

Applying the formulas in the previous subsections, we numerically search for a parameter region which can explain neutrino mass and  $(g - 2)_\mu$  satisfying all the flavor constraints. In our numerical analysis, we have found the following allowed regions to satisfy all the constraints in Eqs. (2.12)–(2.16) and obtain the sizable  $(g - 2)_\mu$  ( $\sim \mathcal{O}(10^{-9})$ ),

$$\begin{aligned} m_{LQ} &\in [1000, 3000] \text{ GeV}, \\ \{m_{DQ}, \mu, m_{Q'}\} &\in [500, 3000] \text{ GeV}, \\ y_L &\in [-0.3, 0.3], \quad Y_2 \in [1, \sqrt{4\pi}], \\ Y_{i \neq 2} &\in [-0.1, 0.1], \end{aligned} \quad (2.22)$$

where three components of  $y_S$  ( $\leq \sqrt{4\pi}$ ) can be solved directly by applying the experimental values of the neutrino oscillations data with the best-fit values in Eq. (2.9).

### III. IMPLICATIONS TO SCALAR SECTOR

In this section, we discuss the effects of the diquark  $S_{DQ}$ , leptoquark  $S_{LQ}$ , and vectorlike quark  $Q'$  to the scalar sector of our model. The diphoton decay of the SM Higgs is discussed for constraining the model, while that of the new neutral scalar boson is analyzed as a possible signature. We also discuss stability of the scalar potential.

#### A. Diphoton decay of SM Higgs

The existence of the leptoquark and diquark can modify the signal strength in SM Higgs measurement. The signal strength parameter is defined by

$$\mu_i^f = \frac{\sigma(pp \rightarrow h)}{\sigma(pp \rightarrow h)_{\text{SM}}} \times \frac{\text{BR}(h \rightarrow f)}{\text{BR}(h \rightarrow f)_{\text{SM}}} \equiv \mu_i \times \mu_f, \quad (3.1)$$

where  $f$  represents the possible channels and  $\mu_i(\mu_f)$  stands for the signal strength of production (decay). Here, we focus on the gluon-gluon fusion (ggF) production and discuss the effects of the leptoquark and diquark on the production and diphoton decay branching ratio (BR).

The leptoquark and diquark contribute to ggF and diphoton decay of the SM Higgs via the following interactions in the potential:

$$\begin{aligned} V &\supset \lambda_{DQ}(\Phi^\dagger \Phi)(S_{DQ}^\dagger S_{DQ}) + \lambda_{LQ}(\Phi^\dagger \Phi)(S_{LQ}^\dagger S_{LQ}) \\ &\supset \lambda_{DQ}vh(S_{DQ}^\dagger S_{DQ}) + \lambda_{LQ}vh(S_{LQ}^\dagger S_{LQ}). \end{aligned} \quad (3.2)$$

Then, loop-induced effective coupling for  $ggh$  is given by

$$\mathcal{L}_{ggh} = -\frac{\alpha_s}{8\pi} \left( \frac{5\mu_{DQ}}{2m_{DQ}^2} A_0(\xi_{DQ}) + \frac{\mu_{LQ}}{2m_{LQ}^2} A_0(\xi_{LQ}) \right) h G^{a\mu\nu} G_\mu^a, \quad (3.3)$$

where  $\xi_X = 4m_X^2/m_h^2$  with  $X = \{LQ, DQ, Q'\}$  and the factor 5 in the first term inside the brackets comes from the Casimir operator for **6** representation. The loop function associated with the scalar is

$$A_0(x) = x(1 - xf(x)), \quad (3.4)$$

with  $f(x) = [\sin^{-1}(1/\sqrt{x})]^2$  for  $x > 1$ . Accordingly, we obtain the signal strength of the gluon fusion Higgs production and decay to the diphoton such that

$$\begin{aligned} \mu_i &= \left| 1 + \frac{v}{A_{1/2}(\xi_t)} \left( \frac{5\lambda_{DQ}v}{m_{DQ}^2} A_0(\xi_{DQ}) + \frac{\lambda_{LQ}v}{m_X^2} A_0(\xi_{LQ}) \right) \right|^2, \\ \mu_{\gamma\gamma} &= \left| 1 + \frac{v^2 N'_c (4/9) A_0(\xi_{DQ}) \lambda_{DQ}/m_{DQ}^2 + N_c (1/9) A_0(\xi_{LQ}) \lambda_{LQ}/m_{LQ}^2}{A_1(\xi_W) + Q_t^2 N_c A_{1/2}(\xi_t)} \right|^2, \end{aligned} \quad (3.5)$$

where  $N_c(N'_c) = 3(6)$  is the number of colors for **3(6)**,  $Q_{DQ}^2 = 4/9$  and  $Q_{LQ}^2 = 1/9$  are used, and the functions for vector-boson and fermion loops are given by

$$\begin{aligned} A_{1/2}(x) &= -2[x + (1-x)f(x)], \\ A_1(x) &= 2 + 3x + 3(2x - x^2)f(x). \end{aligned} \quad (3.6)$$

In our analysis, we set  $\lambda_{DQ} = \lambda_{LQ}$  and  $m_{DQ} = m_{LQ}$  since the effects of the diquark and leptoquark are similar, for simplicity. The  $\mu_i^{\gamma\gamma}$  as a function of  $m_{DQ}$ (=  $m_{LQ}$ ) is shown in Fig. 1(a), and that of  $\lambda_{DQ}$ (=  $\lambda_{LQ}$ ) is presented in Fig. 1(b), where the curves in plot (a) are  $\lambda_{DQ} = \lambda_{LQ} = \{1.0, 3.0, 5.0\}$  and those in plot (b) are  $m_{DQ} = m_{LQ} = \{1.0, 1.1, 1.2\}$  TeV. For comparison, we also indicate the results of ATLAS [48] and CMS [49] with  $1\sigma$  errors in the plots. From the plots, it can be clearly seen that with  $\lambda_{DQ(LQ)}$  of  $\mathcal{O}(1)$  the diquark (leptoquark) contributions can significantly shift the  $\mu_i^{\gamma\gamma}$  away from the SM prediction and that the results are consistent with the current data.

#### B. Exotic diphoton resonance search

Here, we discuss an exotic diphoton resonance as a signature of our model where we consider the singlet scalar field  $\phi$  for illustration; in our following analysis, we set  $m_\phi = 750$  GeV since this point is well investigated. Then, we focus on the trilinear couplings of  $S_{LQ}(S_{DQ})$  and the Yukawa coupling of  $Q'$  associated with  $\phi$ , which are given by

$$\begin{aligned} V &\supset \lambda_{DQ\phi}\phi^2(S_{DQ}^\dagger S_{DQ}) + \lambda_{LQ\phi}\phi^2(S_{LQ}^\dagger S_{LQ}) \\ &\quad + \tilde{\mu}_{DQ\phi}\phi(S_{DQ}^\dagger S_{DQ}) + \tilde{\mu}_{LQ\phi}\phi(S_{LQ}^\dagger S_{LQ}) \\ &\supset \lambda_{DQ\phi}v_\phi\phi(S_{DQ}^\dagger S_{DQ}) + \lambda_{LQ\phi}v_\phi\phi(S_{LQ}^\dagger S_{LQ}) \\ &\quad + \frac{\tilde{\mu}_{DQ\phi}}{\sqrt{2}}\phi(S_{DQ}^\dagger S_{DQ}) + \frac{\tilde{\mu}_{LQ\phi}}{\sqrt{2}}\phi(S_{LQ}^\dagger S_{LQ}) \\ &\equiv \mu_{DQ}\phi(S_{DQ}^\dagger S_{DQ}) + \mu_{LQ}\phi(S_{LQ}^\dagger S_{LQ}), \end{aligned} \quad (3.7)$$

$$L_Y = y_{Q'}\phi\bar{Q}'Q, \quad (3.8)$$

where these interactions contribute to gluon fusion and the diphoton decay processes of  $\phi$  via  $S_{LQ}$ ,  $S_{DQ}$ , and  $Q'$  loops.

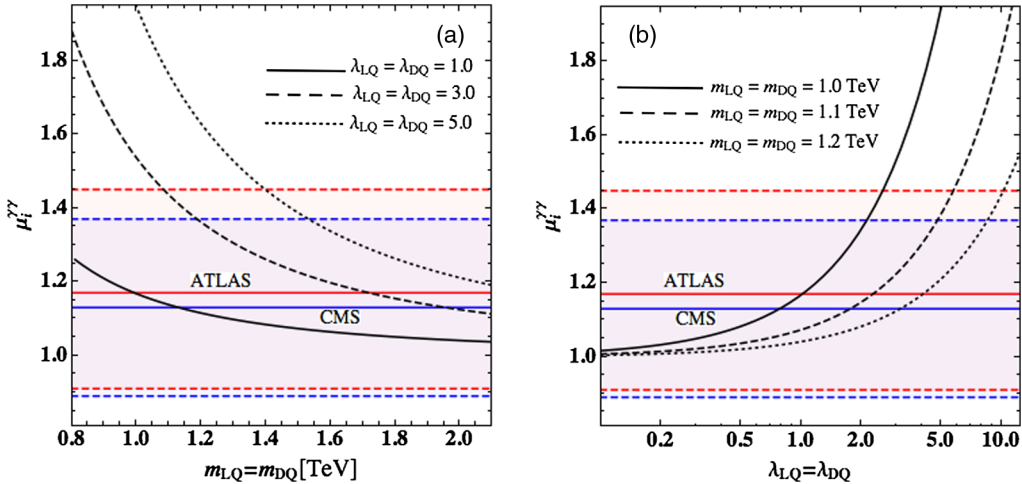


FIG. 1. Diphoton signal strength parameter  $\mu_i^{\gamma\gamma}$  as a function of (a)  $m_{LQ} = m_{DQ}$  and (b)  $\lambda_{LQ} = \lambda_{DQ}$ , where the curves in plots (a) and (b) denote  $\mu_{LQ} = (1.0, 3.0, 5.0)$  TeV and  $m_{LQ} = (1.0, 1.1, 1.2)$  TeV, respectively. The colored region indicates the observed value by ATLAS and CMS within  $1\sigma$  error.

The loop-induced effective coupling for  $gg\phi$  can be written as

$$\mathcal{L}_{gg\phi} = -\frac{\alpha_s}{8\pi} \left( \frac{5\mu_{DQ}}{2m_{DQ}^2} A_0(\tau_{DQ}) + \frac{\mu_{LQ}}{2m_{LQ}^2} A_0(\tau_{LQ}) + \frac{y}{2m_{Q'}^2} A_{1/2}(\tau_{Q'}) \right) \phi G^{\mu\nu} G_{\mu\nu}^a, \quad (3.9)$$

where  $\tau_X = 4m_X^2/m_\phi^2$  with  $X = \{LQ, DQ, Q'\}$  and the factor 5 in the first term inside the brackets is the same as in Eq. (3.3).

The diphoton decay  $S \rightarrow \gamma\gamma$  is dominantly induced by charged leptoquark, diquark, and vectorlike quark loops where the partial decay width is given by

$$\Gamma_{\phi \rightarrow \gamma\gamma} = \frac{\alpha^2 m_\phi^3}{256\pi^3} \left| \frac{8}{3} \frac{\mu_{DQ}}{2m_{DQ}^2} A_0(\tau_{DQ}) + \frac{1}{3} \frac{\mu_{LQ}}{2m_{LQ}^2} A_0(\tau_{LQ}) + \frac{16}{3} \frac{y_{Q'}}{m_{Q'}^2} A_{1/2}(\tau_{Q'}) \right|^2, \quad (3.10)$$

where color factors  $N_c = 6$  and 3 are used for the diquark and leptoquark, respectively. We also obtain the partial decay width for  $S \rightarrow gg$  from effective interaction in Eq. (3.7):

$$\Gamma_{\phi \rightarrow gg} = \frac{\alpha_s^2 m_\phi^2}{32\pi^3} \left| \frac{5\mu_{DQ}}{2m_{DQ}^2} A_0(\tau_{DQ}) + \frac{\mu_{LQ}}{2m_{LQ}^2} A_0(\tau_{LQ}) + \frac{y_{Q'}}{2m_{Q'}^2} A_{1/2}(\tau_{Q'}) \right|^2. \quad (3.11)$$

The total decay width is dominantly obtained from the  $\phi \rightarrow gg$  mode assuming  $\lambda_{H\phi} \ll 1$  to suppress the branching fraction for  $\phi \rightarrow hh$ .

In the narrow-width approximation, the cross section for the process  $gg \rightarrow \phi \rightarrow \gamma\gamma$  can be expressed as [20]

$$\sigma(gg \rightarrow \phi \rightarrow \gamma\gamma) \simeq \frac{C_{gg}}{s} \frac{\Gamma_{\phi \rightarrow gg}}{m_\phi} \text{BR}(\phi \rightarrow \gamma\gamma), \quad (3.12)$$

where  $C_{gg}$  is related to the gluon luminosity function,  $s$  is the center of energy, and  $\text{BR}(\phi \rightarrow \gamma\gamma)$  is the branching fraction of  $\phi \rightarrow \gamma\gamma$  decay. For  $\sqrt{s} = 13$  TeV, we adopt  $C_{gg} \simeq 2137$ . In addition, we use the K-factor for the gluon fusion production process as  $K_{gg} \simeq 1.5$  [20]. For the current constraint for diphoton resonance at  $m_\phi = 750$  GeV, we adopt

$$\sigma(gg \rightarrow \phi \rightarrow \gamma\gamma) \leq 1.2 \text{ fb}, \quad (3.13)$$

taking into account  $1\sigma$  error of ATLAS data. [53]. In Fig. 2, we show the contours of the cross section in the  $\mu$ - $y_{Q'}$  and  $m_{LQ(DQ)}-m_{Q'}$  planes, where we take  $\mu \equiv \mu_{LQ} = \mu_{DQ}$  and fix some parameters as indicated in the plots. We find that the current constraint can exclude some parameter space, and further regions will be tested with future experimental data.

### C. Stability of the potential

It is worth mentioning the vacuum stability for pure quartic couplings of the charged bosons  $\lambda_{LQ}$  and  $\lambda_{DQ}$ . We have a one-loop correction mediated by bosons, which arises from  $\mu_{\varphi LQ}(\varphi S_{LQ}^* S_{LQ})$  and  $\mu_{\varphi DQ}(\varphi S_{DQ}^* S_{DQ})$ , as follows:

$$\lambda_{LQ}^{\text{one-loop}} \approx \lambda_{LQ}^{\text{tree}} - \frac{\mu_{\varphi LQ}^4}{(4\pi)^2} \int_0^1 dx \frac{x(1-x)}{[xm_{LQ}^2 + (1-x)m_\varphi^2]^2}, \quad (3.14)$$

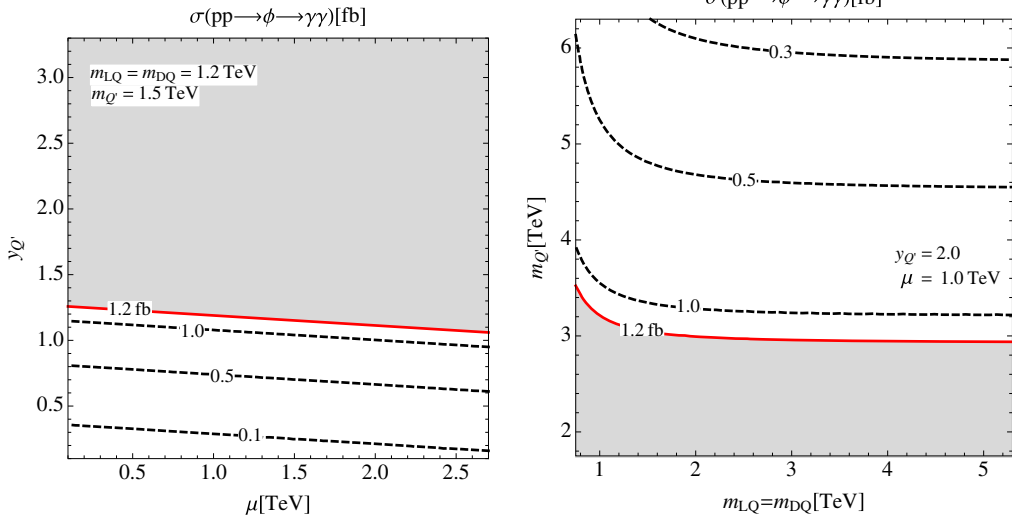


FIG. 2. The cross section for  $pp \rightarrow \phi \rightarrow \gamma\gamma$  in the  $\mu$ - $y_{Q'}$  plane (left) and  $m_{LQ(DQ)}$ - $m_{Q'}$  plane (right) where gray colored regions are excluded by ATLAS data.

$$\lambda_{DQ}^{\text{one-loop}} \approx \lambda_{DQ}^{\text{tree}} - \frac{\mu_{\phi DQ}^4}{(4\pi)^2} \int_0^1 dx \frac{x(1-x)}{[xm_{DQ}^2 + (1-x)m_\phi^2]^2}. \quad (3.15)$$

And each couplings has to satisfy the following condition:

$$0 \lesssim \lambda_{LQ}^{\text{one-loop}} (\lesssim 4\pi), \quad (3.16)$$

$$0 \lesssim \lambda_{DQ}^{\text{one-loop}} (\lesssim 4\pi). \quad (3.17)$$

Here, we estimate the scale of pure couplings under the benchmark points  $m_{LQ} = m_{DQ} = m_\phi = (1, 1.1, 1.2)$  TeV with  $1 \text{ TeV} \leq (\mu_{LQ}, \mu_{DQ}) \leq 5 \text{ TeV}$ . Then, the formulas can be simplified as  $\lambda_{LQ}^{\text{one-loop}} \approx \lambda_{LQ}^{\text{tree}} - \mu_{\phi LQ}^4 / (96\pi^2 m_{LQ}^4)$  and  $\lambda_{DQ}^{\text{one-loop}} \approx \lambda_{DQ}^{\text{tree}} - \mu_{\phi DQ}^4 / (96\pi^2 m_{DQ}^4)$ . Thus, the lower and upper bounds on the pure couplings at tree level can be obtained by

$$m_{LQ} = m_{DQ} = 1000 \text{ GeV} : 1.06 \times 10^{-3} \lesssim \lambda_{LQ(DQ)}^{\text{tree}} \lesssim 0.66, \quad (3.18)$$

$$m_{LQ} = m_{DQ} = 1100 \text{ GeV} : 7.20 \times 10^{-4} \lesssim \lambda_{LQ(DQ)}^{\text{tree}} \lesssim 0.45, \quad (3.19)$$

$$m_{LQ} = m_{DQ} = 1200 \text{ GeV} : 5.10 \times 10^{-4} \lesssim \lambda_{LQ(DQ)}^{\text{tree}} \lesssim 0.318. \quad (3.20)$$

#### IV. IMPLICATIONS TO COLLIDER PHYSICS

In this section, we explore the implications of our model in collider physics. In our analysis, we focus on the

signature of  $Q'$  production, which provides a specific signal of our model.

Here, we discuss the production of  $Q'$  at the collider, since  $Q'$  has an interesting decay mode;  $Q' \rightarrow (\ell) + S_{LQ} \rightarrow \ell + u_i$  through the Yukawa interactions associated with  $Y_i$  and  $y_{L(R)}$ . Since we have some freedom to chose  $y_R$  while satisfying neutrino mass and flavor-violating constraints, we assume here the BRs for  $S_{LQ} \rightarrow \ell u_i$  are universal for  $\ell = e, \mu$  and  $u_i = u, c$ , while the BRs for the other modes are negligibly small. On the other hand, the  $Y_2$  is expected to be dominant to obtain sizable  $(g-2)_\mu$  while avoiding the LFV constraints. Thus,  $Q'$  dominantly decays into a leptoquark and muon. The  $Q'$  pair is produced via the QCD process. We estimate the production cross section with the use of CalcHEP [54], implementing relevant interactions and applying the CTEQ6L parton distribution function (PDF)

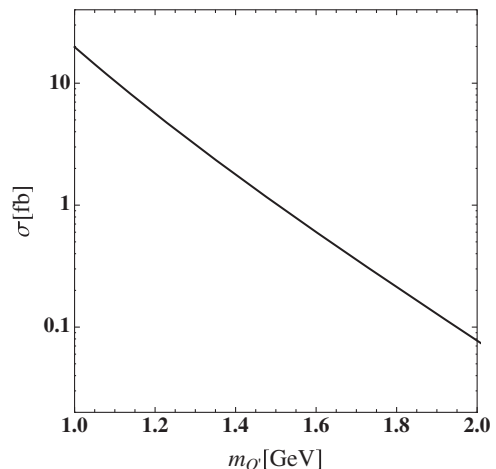


FIG. 3. The cross section for  $pp \rightarrow \bar{Q}'Q'$  at the LHC 13 TeV as a function of  $m_{Q'}$ .

TABLE III. The number of events for signal and backgrounds after kinematical cuts with the luminosity of  $100 \text{ fb}^{-1}$  at the LHC 13 TeV. The significance is also shown in the last column.

	Signal ( $m_{Q'} = 1.5 \text{ TeV}$ )	$ZZj$	$ZZjj$	$Z\bar{t}t$	$ZZW^\pm$	$S$
# of signal events (basic cuts)	103.	$2.28 \times 10^3$	$1.11 \times 10^3$	177.	7.98	1.72
# of signal events with Eq. (4.3)	93.2	0.84	0.96	3.54	<0.1	40.3

[55] in the estimation. In Fig. 3, we show the production at the LHC 13 TeV as a function of  $Q'$  mass  $m_{Q'}$ .

We then carry out simple simulation at the parton level with the event generator MADGRAPH/MADEVENT 5 [56], where the necessary Feynman rules and relevant parameters of the model are implemented by the use of FeynRules 2.0 [57] and the NNPDF23LO1 PDF [58] is adopted. For a signal, we generate the events for the process

$$pp \rightarrow \bar{Q}'Q' \rightarrow S_{LQ}S_{LQ}^* \ell^+\ell^- \rightarrow \ell^+\ell^+\ell^-\ell^- jj. \quad (4.1)$$

Thus, our signal includes four leptons and two jets:  $4\ell+2j$ . We then select the events as four-leptons and jet(s) where the number of jets is required to be  $n_j \geq 1$ . For the SM backgrounds, we consider SM processes producing  $ZZj$ ,  $ZZjj$ ,  $t\bar{t}Z$ , and  $ZZW^\pm$ , which can provide the four-leptons plus jet(s) final states if  $Z$  and  $W^\pm$  decay into leptons and jets, respectively. In generating the events, the basic cuts

$$\begin{aligned} p_T(\ell) &> 10 \text{ GeV}, & p_T(j) &> 20 \text{ GeV}, \\ \eta(\ell) &> 2.5, & \eta(j) &> 5 \end{aligned} \quad (4.2)$$

are adopted, where  $p_T$  and  $\eta$  are the transverse momentum and pseudorapidity, respectively. In addition, we apply selecting cuts of

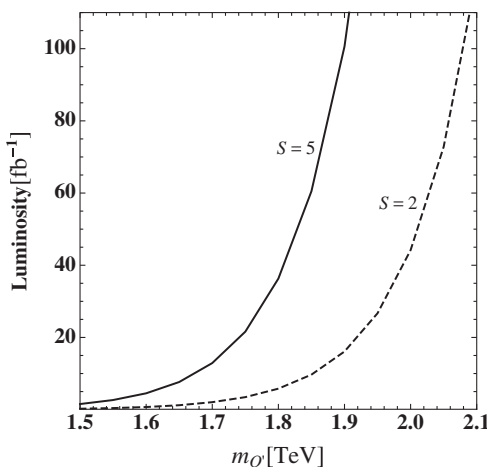


FIG. 4. The luminosity required to obtain significance 5(2) shown as a solid (dashed) line.

$$\begin{aligned} p_T(\ell_{\text{leading}}) &> 50 \text{ GeV}, & P_T(j_{\text{leading}}) &> 100 \text{ GeV}, \\ m_Z - 10 \text{ GeV} < M_{\ell^+\ell^-} < m_Z + 10 \text{ GeV} & \text{(veto)}, \end{aligned} \quad (4.3)$$

where  $\ell_{\text{leading}}$  ( $j_{\text{leading}}$ ) are leading lepton (jet), and the second line is for vetoing the region of  $m_Z \pm 10$  for the invariant mass  $M_{\ell^+\ell^-}$ . Then, we estimate the significance for the signal by

$$S = \frac{N_S}{\sqrt{N_B}}, \quad (4.4)$$

where  $N_S$  and  $N_B$  are the number of signal and background events, respectively. In Table III, we show the number of events with basic cuts and after the cuts in Eq. (4.3) for signal with  $m_{Q'} = 1.5 \text{ TeV}$  and SM backgrounds using a luminosity of  $100 \text{ fb}^{-1}$ . We find that the vetoing condition for  $M_{\ell^+\ell^-}$  highly suppress the SM backgrounds and the large significance can be achieved. The luminosity required to obtain  $S = 5(2)$  is also shown in Fig. 4 as a function of  $m_{Q'}$ . We see that the significance of 5(2) that can be reached for  $Q'$  mass  $m_{Q'} \lesssim 1.9(2.1) \text{ TeV}$  could be tested at the LHC 13 TeV with the integrated luminosity of  $100 \text{ fb}^{-1}$ . In addition, the signature of  $Q'$  can be seen as a bump in the distribution of the invariant mass for two same-sign lepton plus jets. Note that, taking into account the detector efficiency, the significance will be smaller, but our result is still a reasonable estimation.

## V. CONCLUSIONS AND DISCUSSIONS

In this paper, we have discussed the extended colored Zee-Babu model in which an isosinglet vectorlike quark and singlet scalar were included to accommodate  $(g-2)_\mu$ . Then, the active neutrino mass matrix and  $(g-2)_\mu$ , which were induced at the two-loop and one-loop levels, respectively, were analyzed. We also took into account the flavor-changing neutral current to check the consistency with experimental constraints. Our analysis has shown that neutrino mass matrix and  $(g-2)_\mu$  can be fitted with experimental data satisfying the constraints.

The implications to the scalar sector such as the decay of the SM Higgs, exotic diphoton resonance, and scalar potential have been discussed. We have shown that exotic colored/charged particles can shift the signal strength for  $h \rightarrow \gamma\gamma$ , which could be tested by the LHC experiments.

Furthermore, exotic diphoton resonance can be a good probe of our model since we expect such a signal from some exotic neutral scalar boson interacting with the diquark, leptoquark, and vectorlike quark in the model. We have shown that a sizable cross section for diphoton resonance production can be obtained in the model, which is compared with the current LHC constraint.

Then, we explored collider physics in our model focusing on the vectorlike quark signature. The vectorlike quarks were produced via the QCD process and decayed into a lepton and leptoquark, which decayed into a lepton and jet. Thus, the signal of vectorlike quark pair production was

four-leptons plus jets. We then estimated the production cross section and carried out a simple simulation study including the SM background. By adopting some kinematical cuts, we have shown the vectorlike quark, which has mass  $m_{Q'} \lesssim 2$  TeV, can be tested at the LHC 13 TeV with integrated luminosity  $100 \text{ fb}^{-1}$ .

## ACKNOWLEDGMENTS

The authors would like thank Dr. Masaya Kohda for fruitful discussions. H. O. is sincerely grateful for all the KIAS members.

- 
- [1] A. Zee, *Phys. Lett.* **93B**, 389 (1980); **95B**, 290 (1980); T. P. Cheng and , *Phys. Rev. D* **22**, 2860 (1980); L. F. LiE. Ma, *Phys. Rev. D* **73**, 077301 (2006).
- [2] A. Zee, *Nucl. Phys.* **B264**, 99 (1986); K. S. Babu, *Phys. Lett. B* **203**, 132 (1988).
- [3] L. M. Krauss, S. Nasri, and M. Trodden, *Phys. Rev. D* **67**, 085002 (2003); M. Aoki, S. Kanemura, and O. Seto, *Phys. Rev. Lett.* **102**, 051805 (2009); M. Gustafsson, J. M. No, and M. A. Rivera, *Phys. Rev. Lett.* **110**, 211802 (2013).
- [4] B. S. Balakrishna, *Phys. Rev. Lett.* **60**, 1602 (1988); B. S. Balakrishna and R. N. Mohapatra, *Phys. Lett. B* **216**, 349 (1989); X. G. He, R. R. Volkas, and D. D. Wu, *Phys. Rev. D* **41**, 1630 (1990); T. Hambye, K. Kannike, E. Ma, and M. Raidal, *Phys. Rev. D* **75**, 095003 (2007); P.-H. Gu and U. Sarkar, *Phys. Rev. D* **77**, 105031 (2008); N. Sahu and U. Sarkar, *Phys. Rev. D* **78**, 115013 (2008); P.-H. Gu and U. Sarkar, *Phys. Rev. D* **78**, 073012 (2008); D. Aristizabal Sierra and D. Restrepo, *J. High Energy Phys.* **08** (2006) 036; R. Bouchand and A. Merle, *J. High Energy Phys.* **07** (2012) 084; K. L. McDonald, *J. High Energy Phys.* **11** (2013) 131; E. Ma, *Phys. Lett. B* **732**, 167 (2014); Y. Kajiyama, H. Okada, and K. Yagyu, *Nucl. Phys.* **B887**, 358 (2014); S. Kanemura, O. Seto, and T. Shimomura, *Phys. Rev. D* **84**, 016004 (2011); S. Kanemura, T. Nabeshima, and H. Sugiyama, *Phys. Lett. B* **703**, 66 (2011); S. Kanemura, T. Nabeshima, and H. Sugiyama, *Phys. Rev. D* **85**, 033004 (2012); D. Schmidt, T. Schwetz, and T. Toma, *Phys. Rev. D* **85**, 073009 (2012); S. Kanemura and H. Sugiyama, *Phys. Rev. D* **86**, 073006 (2012); Y. Farzan and E. Ma, *Phys. Rev. D* **86**, 033007 (2012); K. Kumericki, I. Picek, and B. Radovcic, *J. High Energy Phys.* **07** (2012) 039; K. Kumericki, I. Picek, and B. Radovcic, *Phys. Rev. D* **86**, 013006 (2012); E. Ma, *Phys. Lett. B* **717**, 235 (2012); G. Gil, P. Chankowski, and M. Krawczyk, *Phys. Lett. B* **717**, 396 (2012); H. Okada and T. Toma, *Phys. Rev. D* **86**, 033011 (2012); D. Hehn and A. Ibarra, *Phys. Lett. B* **718**, 988 (2013); P. S. B. Dev and A. Pilaftsis, *Phys. Rev. D* **86**, 113001 (2012); Y. Kajiyama, H. Okada, and T. Toma, *Eur. Phys. J. C* **73**, 2381 (2013); S. Kanemura, T. Matsui, and H. Sugiyama, *Phys. Lett. B* **727**, 151 (2013); S. S. C. Law and K. L. McDonald, *J. High Energy Phys.* **09** (2013) 092; B. Dasgupta, E. Ma, and K. Tsumura, *Phys. Rev. D* **89**, 041702 (2014); S. Baek and H. Okada, [arXiv:1403.1710](#); S. Kanemura, T. Matsui, and H. Sugiyama, *Phys. Rev. D* **90**, 013001 (2014); S. Fraser, E. Ma, and O. Popov, *Phys. Lett. B* **737**, 280 (2014); S. Baek, H. Okada, and K. Yagyu, *J. High Energy Phys.* **04** (2015) 049; D. Restrepo, A. Rivera, M. Sánchez-Peláez, O. Zapata, and W. Tangarife, [arXiv:1504.07892](#); W. Wang and Z. L. Han, *Phys. Rev. D* **92**, 095001 (2015); Y. H. Ahn and H. Okada, *Phys. Rev. D* **85**, 073010 (2012); E. Ma, A. Natale, and A. Rashed, *Int. J. Mod. Phys. A* **27**, 1250134 (2012); A. E. Carcamo Hernandez, I. d. M. Varzielas, S. G. Kovalenko, H. Pás, and I. Schmidt, *Phys. Rev. D* **88**, 076014 (2013); E. Ma and A. Natale, *Phys. Lett. B* **734**, 403 (2014); E. Ma, *Phys. Lett. B* **741**, 202 (2015); E. Ma, [arXiv:1504.02086](#); E. Ma, *Phys. Rev. Lett.* **112**, 091801 (2014); H. Okada and K. Yagyu, *Phys. Rev. D* **89**, 053008 (2014); H. Okada and K. Yagyu, *Phys. Rev. D* **90**, 035019 (2014); V. Brdar, I. Picek, and B. Radovcic, *Phys. Lett. B* **728**, 198 (2014); H. Okada, Y. Orikasa, and T. Toma, [arXiv:1511.01018](#); F. Bonnet, M. Hirsch, T. Ota, and W. Winter, *J. High Energy Phys.* **07** (2012) 153; H. Davoudiasl and I. M. Lewis, *Phys. Rev. D* **90**, 033003 (2014); M. Lindner, S. Schmidt, and J. Smirnov, [arXiv:1405.6204](#); H. Okada and Y. Orikasa, [arXiv:1412.3616](#); Y. Mambrini, S. Profumo, and F. S. Queiroz, [arXiv:1508.06635](#); S. M. Boucenna, S. Morisi, and J. W. F. Valle, *Adv. High Energy Phys.* **2014**, 831598 (2014); A. Ahriche, S. M. Boucenna, and S. Nasri, [arXiv:1601.04336](#); S. Fraser, C. Kownacki, E. Ma, and O. Popov, [arXiv:1511.06375](#); S. Fraser, E. Ma, and M. Zakeri, [arXiv:1511.07458](#); R. Adhikari, D. Borah, and E. Ma, [arXiv:1512.05491](#); H. Okada and Y. Orikasa, [arXiv:1512.06687](#); C. Arbelaez, A. E. C. Hernandez, S. Kovalenko, and I. Schmidt, [arXiv:1602.03607](#); A. Ahriche, K. L. McDonald, S. Nasri, and I. Picek, *Phys. Lett. B* **757**, 399 (2016); W. B. Lu and P. H. Gu, [arXiv:1603.05074](#); C. Kownacki and E. Ma, [arXiv:1604.01148](#); A. Ahriche, K. L. McDonald, and S. Nasri, [arXiv:1604.05569](#); A. Ahriche, A. Manning, K. L. McDonald, and S. Nasri, [arXiv:1604.05995](#); E. Ma, N. Pollard, O. Popov, and M. Zakeri, [arXiv:1605.00991](#); T. Nomura, H. Okada, and Y. Orikasa, [arXiv:1605.02601](#);

- C. Hagedorn, T. Ohlsson, S. Riad, and M. A. Schmidt, arXiv:1605.03986; O. Antipin, P. Culjak, K. Kumericki, and I. Picek, arXiv:1606.05163; T. Nomura and H. Okada, arXiv:1606.09055; A. E. Carcamo Hernandez, arXiv: 1512.09092.
- [5] K. S. Babu and C. Macesanu, Phys. Rev. D **67**, 073010 (2003); M. Nebot, J. F. Oliver, D. Palao, and A. Santamaria, Phys. Rev. D **77**, 093013 (2008); D. Schmidt, T. Schwetz, and H. Zhang, Nucl. Phys. **B885**, 524 (2014); J. Herrero-Garcia, M. Nebot, N. Rius, and A. Santamaria, Nucl. Phys. **B885**, 542 (2014); H. N. Long and V. V. Vien, Int. J. Mod. Phys. A **29**, 1450072 (2014); V. Van Vien, H. N. Long, and P. N. Thu, arXiv:1407.8286; M. Aoki, S. Kanemura, T. Shindou, and K. Yagyu, J. High Energy Phys. 07 (2010) 084; 1011, 049 (2010); M. Lindner, D. Schmidt, and T. Schwetz, Phys. Lett. B **705**, 324 (2011); S. Baek, P. Ko, H. Okada, and E. Senaha, J. High Energy Phys. 09 (2014) 153; M. Aoki, J. Kubo, and H. Takano, Phys. Rev. D **87**, 116001 (2013); Y. Kajiyama, H. Okada, and K. Yagyu, Nucl. Phys. **B874**, 198 (2013); Y. Kajiyama, H. Okada, and T. Toma, Phys. Rev. D **88**, 015029 (2013); S. Baek, H. Okada, and T. Toma, J. Cosmol. Astropart. Phys. 06 (2014) 027; H. Okada, arXiv:1404.0280; H. Okada, T. Toma, and K. Yagyu, Phys. Rev. D **90**, 095005 (2014); H. Okada, arXiv:1503.04557; C. Q. Geng and L. H. Tsai, arXiv:1503.06987; S. Kashiwase, H. Okada, Y. Oriksa, and T. Toma, arXiv: 1505.04665; M. Aoki and T. Toma, J. Cosmol. Astropart. Phys. 09 (2014) 016; S. Baek, H. Okada, and T. Toma, Phys. Lett. B **732**, 85 (2014); H. Okada and Y. Oriksa, arXiv:1509.04068; D. Aristizabal Sierra, A. Degee, L. Dorame, and M. Hirsch, J. High Energy Phys. 03 (2015) 040; T. Nomura and H. Okada, Phys. Lett. B **756**, 295 (2016); T. Nomura, H. Okada, and Y. Oriksa, arXiv: 1602.08302.
- [6] A. Ahriche, S. Nasri, and R. Soualah, Phys. Rev. D **89**, 095010 (2014); A. Ahriche, C. S. Chen, K. L. McDonald, and S. Nasri, Phys. Rev. D **90**, 015024 (2014); A. Ahriche, K. L. McDonald, and S. Nasri, J. High Energy Phys. 10 (2014) 167; C.-S. Chen, K. L. McDonald, and S. Nasri, Phys. Lett. B **734**, 388 (2014); H. Okada and Y. Oriksa, Phys. Rev. D **90**, 075023 (2014); H. Hatanaka, K. Nishiwaki, H. Okada, and Y. Oriksa, Nucl. Phys. **B894**, 268 (2015); L. G. Jin, R. Tang, and F. Zhang, Phys. Lett. B **741**, 163 (2015); P. Culjak, K. Kumericki, and I. Picek, Phys. Lett. B **744**, 237 (2015); H. Okada, N. Okada, and Y. Oriksa, Phys. Rev. D **93**, 073006 (2016); C. Q. Geng, D. Huang, and L. H. Tsai, Phys. Lett. B **745**, 56 (2015); A. Ahriche, K. L. McDonald, S. Nasri, and T. Toma, Phys. Lett. B **746**, 430 (2015); K. Nishiwaki, H. Okada, and Y. Oriksa, arXiv:1507.02412; H. Okada and K. Yagyu, arXiv: 1508.01046; A. Ahriche, K. L. McDonald, and S. Nasri, arXiv:1508.02607; Y. Kajiyama, H. Okada, and K. Yagyu, J. High Energy Phys. 10 (2013) 196; S. F. King, A. Merle, and L. Panizzi, arXiv:1406.4137; H. Okada and K. Yagyu, Phys. Lett. B **756**, 337 (2016); P. Ko, T. Nomura, H. Okada, and Y. Oriksa, arXiv:1602.07214; T. Nomura, H. Okada, and Y. Oriksa, arXiv:1603.04631; T. T. Thuc, L. T. Hue, H. N. Long, and T. P. Nguyen, arXiv:1604.03285; D. Cherigui, C. Guella, A. Ahriche, and S. Nasri, arXiv: 1605.03640.
- [7] T. Nomura and H. Okada, Phys. Lett. B **755**, 306 (2016).  
[8] T. Nomura and H. Okada, arXiv:1601.04516.  
[9] M. Aaboud *et al.* (ATLAS Collaboration), J. High Energy Phys. 09 (2016) 001.  
[10] V. Khachatryan *et al.* (CMS Collaboration), Phys. Rev. Lett. **117**, 051802 (2016).  
[11] K. Harigaya and Y. Nomura, Phys. Lett. B **754**, 151 (2016).  
[12] Y. Mambrini, G. Arcadi, and A. Djouadi, Phys. Lett. B **755**, 426 (2016).  
[13] M. Backovic, A. Mariotti, and D. Redigolo, J. High Energy Phys. 03 (2016) 157.  
[14] A. Angelescu, A. Djouadi, and G. Moreau, Phys. Lett. B **756**, 126 (2016).  
[15] Y. Nakai, R. Sato, and K. Tobioka, Phys. Rev. Lett. **116**, 151802 (2016).  
[16] D. Buttazzo, A. Greljo, and D. Marzocca, Eur. Phys. J. C **76**, 116 (2016).  
[17] S. Di Chiara, L. Marzola, and M. Raidal, Phys. Rev. D **93**, 095018 (2016).  
[18] S. Knapen, T. Melia, M. Papucci, and K. Zurek, Phys. Rev. D **93**, 075020 (2016).  
[19] A. Pilaftsis, Phys. Rev. D **93**, 015017 (2016).  
[20] R. Franceschini, G. F. Giudice, J. F. Kamenik, M. McCullough, A. Pomarol, R. Rattazzi, M. Redi, F. Riva, A. Strumia, and R. Torre, J. High Energy Phys. 03 (2016) 144.  
[21] J. Ellis, S. A. R. Ellis, J. Quevillon, V. Sanz, and T. You, J. High Energy Phys. 03 (2016) 176.  
[22] R. S. Gupta, S. Jager, Y. Kats, G. Perez, and E. Stamou, J. High Energy Phys. 07 (2016) 145.  
[23] A. Kobakhidze, F. Wang, L. Wu, J. M. Yang, and M. Zhang, Phys. Lett. B **757**, 92 (2016).  
[24] A. Falkowski, O. Slone, and T. Volansky, J. High Energy Phys. 02 (2016) 152.  
[25] R. Benbrik, C. H. Chen, and T. Nomura, Phys. Rev. D **93**, 055034 (2016).  
[26] R. Ding, L. Huang, T. Li, and B. Zhu, arXiv:1512.06560.  
[27] F. Wang, L. Wu, J. M. Yang, and M. Zhang, Phys. Lett. B **759**, 191 (2016).  
[28] P. S. B. Dev and D. Teresi, Phys. Rev. D **94**, 025001 (2016).  
[29] B. C. Allanach, P. S. B. Dev, S. A. Renner, and K. Sakurai, Phys. Rev. D **93**, 115022 (2016).  
[30] K. Cheung, P. Ko, J. S. Lee, J. Park, and P. Y. Tseng, Phys. Rev. D **94**, 033010 (2016).  
[31] F. Wang, W. Wang, L. Wu, J. M. Yang, and M. Zhang, arXiv:1512.08434.  
[32] X.-J. Bi, R. Ding, Y. Fan, L. Huang, C. Li, T. Li, S. Raza, X.-C. Wang, and B. Zhu, Phys. Rev. D **94**, 015012 (2016).  
[33] C. W. Chiang, M. Ibe, and T. T. Yanagida, J. High Energy Phys. 05 (2016) 084.  
[34] X. J. Huang, W. H. Zhang, and Y. F. Zhou, Phys. Rev. D **93**, 115006 (2016).  
[35] X. F. Han, L. Wang, L. Wu, J. M. Yang, and M. Zhang, Phys. Lett. B **756**, 309 (2016).  
[36] P. Ko, Y. Omura, and C. Yu, J. High Energy Phys. 04 (2016) 098.  
[37] R. Ding, Z. L. Han, Y. Liao, and X. D. Ma, Eur. Phys. J. C **76**, 204 (2016).  
[38] P. Ko and T. Nomura, Phys. Lett. B **758**, 205 (2016).

- [39] I. Dorsner, S. Fajfer, and N. Kosnik, *Phys. Rev. D* **94**, 015009 (2016).
- [40] X. F. Han, L. Wang, and J. M. Yang, *Phys. Lett. B* **757**, 537 (2016).
- [41] P. S. B. Dev, R. N. Mohapatra, and Y. Zhang, *J. High Energy Phys.* **02** (2016) 186.
- [42] S. Kanemura, K. Nishiwaki, H. Okada, Y. Orikasa, S. C. Park, and R. Watanabe, [arXiv:1512.09048](#).
- [43] U. K. Dey, S. Mohanty, and G. Tomar, [arXiv:1606.07903](#).
- [44] CMS Collaboration, Report No. CMS-PAS-EXO-16-027.
- [45] ATLAS Collaboration, Report No. ATLAS-CONF-2016-059.
- [46] V. Khachatryan *et al.* (CMS Collaboration), [arXiv:1609.02507](#).
- [47] M. Kohda, H. Sugiyama, and K. Tsumura, *Phys. Lett. B* **718**, 1436 (2013).
- [48] G. Aad *et al.* (ATLAS Collaboration), *Eur. Phys. J. C* **76**, 6 (2016).
- [49] CMS Collaboration, Report No. CMS-PAS-HIG-14-009.
- [50] D. Aristizabal Sierra and M. Hirsch, *J. High Energy Phys.* **12** (2006) 052.
- [51] D. V. Forero, M. Tortola, and J. W. F. Valle, *Phys. Rev. D* **90**, 093006 (2014).
- [52] M. Carpentier and S. Davidson, *Eur. Phys. J. C* **70**, 1071 (2010).
- [53] ATLAS Collaboration, Report No. ATLAS-CONF-2016-018.
- [54] A. Belyaev, N. D. Christensen, and A. Pukhov, *Comput. Phys. Commun.* **184**, 1729 (2013).
- [55] P. M. Nadolsky, H. L. Lai, Q. H. Cao, J. Huston, J. Pumplin, D. Stump, W. K. Tung, and C.-P. Yuan, *Phys. Rev. D* **78**, 013004 (2008).
- [56] J. Alwall, R. Frederix, S. Frixione, V. Hirschi, F. Maltoni, O. Mattelaer, H.-S. Shao, T. Stelzer, P. Torrielli, and M. Zaro, *J. High Energy Phys.* **07** (2014) 079.
- [57] A. Alloul, N. D. Christensen, C. Degrande, C. Duhr, and B. Fuks, *Comput. Phys. Commun.* **185**, 2250 (2014).
- [58] C. S. Deans (NNPDF Collaboration), [arXiv:1304.2781](#).